Separation and Characterization of Metallosupramolecular Libraries by Ion Mobility Mass Spectrometry

ARTICLE *in* ANALYTICAL CHEMISTRY · AUGUST 2011

Impact Factor: 5.64 · DOI: 10.1021/ac201161u · Source: PubMed

analytical chemistry

ARTICLE

pubs.acs.org/ac

Separation and Characterization of Metallosupramolecular Libraries by Ion Mobility Mass Spectrometry

Xiaopeng Li,[†] Yi-Tsu Chan,[‡] Madalis Casiano-Maldonado,[†] Jing Yu,[‡] Gustavo A. Carri,[‡] George R. Newkome,*[,†,‡] and Chrys Wesdemiotis*[,†,‡]

[†]Departments of Chemistry and [‡]Polymer Science, The University of Akron, Akron, Ohio 44325, United States

Supporting Information

ABSTRACT: The self-assembly of Zn^{II} ions and bis(terpyridine) (tpy) ligands carrying 120° or 180° angles between their metal binding sites was utilized to prepare metallosupramolecular libraries with the <tpy−Zn^{II}−tpy> connectivity. These combinatorial libraries were separated and characterized by ion mobility mass spectrometry (IM MS) and tandem mass spectrometry (MS^2). The 180°-angle building blocks generate exclusively linear complexes, which were used as standards to determine the architectures of the assemblies resulting from the 120°-angle ligands. The latter ligand geometry promotes the formation of macrocyclic hexamers, but other *n*-mers with smaller ($n = 5$) or larger ring sizes ($n = 7-9$) were identified as minor products, indicating that the angles in the bis(terpyridine) ligand and within the coordinative tpy−Zn^{II}−tpy bonds are not as rigid, as previously believed. Macrocyclic and linear isomers were detected in penta- and heptameric assemblies; in the larger octa- and nonameric assemblies, ring-opened conformers with compact and folded geometries were observed in addition to linear extended and cyclic architectures. IM MS^2 experiments provided strong evidence that the macrocycles present in the libraries were already formed in solution, during the self-assembly process, not by dissociation of larger complexes in the gas phase. The IM MS/MS^2 methods provide a means to analyze, based on size and shape (architecture), supramolecular libraries that are not amenable to liquid chromatography, LC-MS, NMR, and/or X-ray techniques.

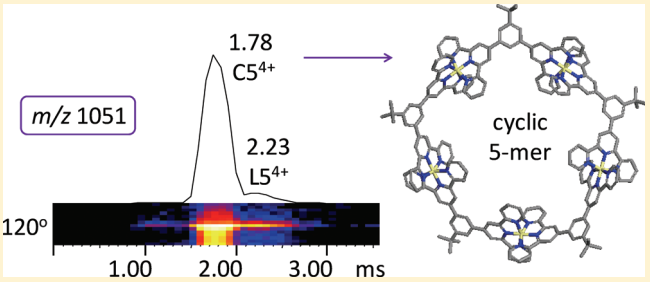

Self-assembling processes based on metal−ligand coordinative interactions often proceed through competing reversible equilibria[1,2] that may lead to mixtures of assemblies with comparable stabilities but different stoichiometries and/or architectures.[1−15] According to Lehn's combinatorial library concept,[6−8,16−18] the corresponding equilibrium positions can be controlled by external factors, such as concentration,[3,9,13] temperature,[19,20] solvent,[14] and counterions or by adding a template molecule to induce and stabilize one particular assembly.[6,8−11] A certain geometry may be promoted by using tailored, rigid building blocks; for example, bis(terpyridine) ligands possessing a 120°-angle between the two ligating sites should preferentially self-assemble to hexameric metallomacrocycles. Indeed, this structure is predominantly formed;[21−24] however, minor products of smaller or larger ring size are coproduced.[25−27] In earlier studies, the nonhexameric sizes escaped detection due to difficulties in separating and conclusively identifying species generated in low concentration and having fairly similar spectral characteristics with the hexamers. Nevertheless, Newkome et al. recently succeeded in isolating, via column chromatography, unexpected pentameric, heptameric, octameric, nonameric, and decameric macrocycles composed of Fe^{II} (or Fe^{II} and Ru^{II}) and rigid bis(terpyridine) ligands with 120°-orientation of their metal binding sites.[25−27] The generation of mixtures during the assembly process offers a means for constructing combinatorial libraries of supramolecular macrocyclic bis(terpyridine) complexes, from which a single member may be isolated for examination of its properties.

This promising approach faces two significant challenges. Few metallomacrocycles are stable enough to sustain chromatographic separation; the particularly high stability of bis(terpyridine) complexes with Fe^{II} and Ru^{II} permitted their fractionation by chromatography techniques (vide supra),[25−27] but similar complexes with many other metals (for example, Cd^{II}, Pd^{II}, or Zn^{II}) largely disintegrate during such extensive purification. Hence, analytical methods capable of characterizing the raw synthetic mixture are necessary, which is impossible with X-ray crystallography and can be problematic with NMR spectroscopy. Electrospray ionization mass spectrometry (ESI MS) would be most suitable for the characterization of metallomacrocyclic combinatorial libraries due to its insensitivity to impurities, dispersive nature, and high sensitivity.

ESI MS already is an essential tool in the determination of supramolecular compositions.[28−37] This method cannot, however, distinguish isomeric structures, even at high mass resolution. Furthermore, weakly bound assemblies tend to form several

Received: May 12, 2011
Accepted: July 11, 2011
Published: July 11, 2011

differently charged fragments, which may overlap with the intact complex at the same mass-to-charge ratio (m/z), thereby hindering definitive compositional assignments. These problems were mostly resolved after the combination of ESI with ion mobility mass spectrometry (IM MS)[38−46] was introduced to supramolecular analysis.[26,27,47−52] IM MS and the closely related variant of traveling wave ion mobility mass spectrometry (TWIM MS)[26,27,44,47−49,51−58] enable mass-, charge-, and shape-dependent dispersion to resolve isomers with distinct architectures as well as to deconvolute the isotope clusters of overlapping charge distributions. Separation is achieved by allowing the ions, formed during ESI, to drift under the influence of an electric field against the stream of a buffer gas. This process resembles a chromatographic fractionation, performed on solitary ions in the gas phase. Although some collision-induced fragmentation may occur in the IM MS experiment, the solvent-free environment and the absence of distribution equilibria with a stationary phase eliminate the risk of bimolecular disintegration reactions, making this method ideally suitable for the analysis of labile or reactive supramolecular assemblies. Here, we report the first IM MS application to supramolecular libraries of self-assembled Zn^{II}−bis(terpyridine) complexes.

EXPERIMENTAL SECTION

Self-Assembly Procedure. All chemicals were purchased from Sigma-Aldrich (St. Louis, MO) or Fisher Scientific (Pittsburgh, PA) and used without further purification. The bis(terpyridine) ligands were synthesized according to our previously reported procedures.[47] Self-assembly was effected by adding a solution of $Zn(OTf)_2$ (17.1 μmol) in MeOH (2 mL) to a stirred solution of ligand (17.1 μmol) in $CHCl_3$ (3 mL). After the reaction mixture was stirred for 1 h at 25 °C, the solvent was evaporated in vacuo. The resulting crude material was used for the mass spectrometric analysis.

Ion Mobility Mass Spectrometry (IM MS). All experiments were performed with a Waters Synapt HDMS quadrupole/time-of-flight (Q/ToF) tandem mass spectrometer equipped with electrospray ionization (ESI).[26,27,47,55,56,58] Experimental details are provided in the Supporting Information. There, we also outline the procedure used to convert ion drift times to experimental collision cross-sections[54] as well as the molecular modeling performed to simulate the collision cross-sections of specific metallosupramolecular architectures.

RESULTS AND DISCUSSION

ESI MS Analysis of Libraries 1 and 2 Reveals Considerable Complexity. In an earlier study,[47] the Cd^{II}-mediated complexation of bis(terpyridine) ligands was found to generate mainly the hexameric macrocycle due to the kinetically labile <tpy−Cd^{II}−tpy> connectivity (log K_1 = 6.33).[59] In contrast, the relatively inert <tpy−Zn^{II}−tpy> bonds (log K_1 = 7.58)[59] afford a distribution of n-mers (n = 5−10) in multiple unique charge states, as attested by the ESI mass spectra of Figure 1 (see Tables S1 and S2 in Supporting Information for the m/z values of the variously charged n-mers). For simplicity, the individual complexes are abbreviated as Mn^{x+}, where M designates the <tpy−Zn^{II}−tpy> repeat unit (with ligand **1** or **2**), n the number of units in the complex, and x the number of positive charges. Although several compositions overlap, the stoichiometries $M6^{5+}$, $M7^{3+}$, $M7^{4+}$, $M8^{3+}$, $M8^{5+}$, $M9^{4+}$, and $M9^{5+}$ are observed at unique m/z ratios

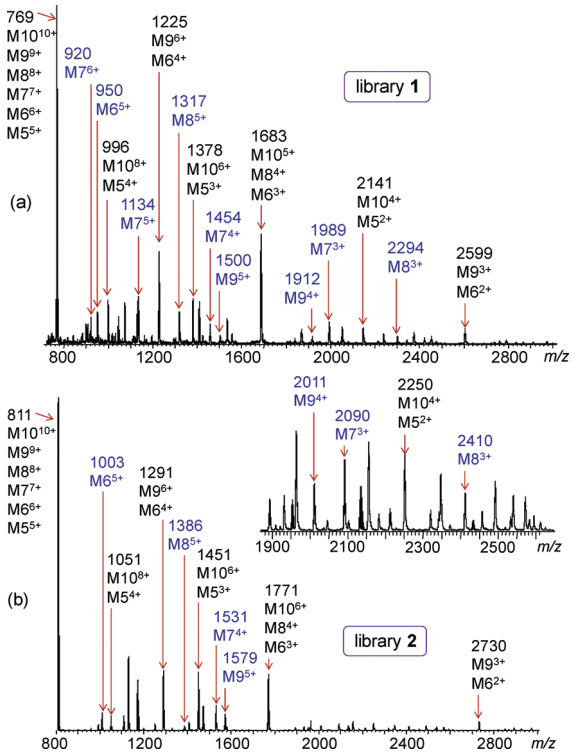

Figure 1. ESI mass spectra of (a) library **1** and (b) library **2**; the labels on top of the peaks give the m/z ratio of the most abundant isotope and the possible ion compositions. Charge states with unique m/z ratios (no overlapping compositions) are labeled in blue.

for library **1** as well as **2** (cf., Figure 1). Considering that only hexazinc macrocycles had been isolated in a previous study about the Zn^{II}-mediated complexation of 120°-juxtaposed terpyridine ligands,[24] a question raised from our current results is whether multiple macrocyclic sizes exist for such Zn^{II}−bis(terpyridine) assemblies. If macrocycle libraries are generated during self-assembly, the IM MS technique provides the opportunity to separate and characterize their constituents. A second question is whether the nonhexameric <tpy−Zn^{II}−tpy> macrocycles are generated in solution, during the self-assembly process or in gas phase (viz., during IM MS analysis). Before these issues are addressed, ions in different charge states from the hexamer (M6) will be examined first by IM MS. Note that the peaks due to M6 ions, both at unique and overlapping m/z values, have high relative intensities, consistent with the hexamer being the major isolated self-assembly product.

Characterization of Differently Charged Hexazinc Macrocycles. The actual composition of a complex with n <tpy−Zn^{II}−tpy> repeat units in charge state x is <tpy−Zn−tpy>$_n$-$(OTf)_{2n-x}^{x+}$ or, based on the symbols introduced above, Mn-$(OTf)_{2n-x}^{x+}$. For brevity, linear and cyclic architectures will be denoted as Ln or Cn, respectively, and the OTf^- counterions will be omitted, as their number is implicitly given by the charge state. Thus, according to this nomenclature, the acronym $L2^{1+}$ represents the linear complex <tpy−Zn−tpy>$_2(OTf)_3^{1+}$ with the overall composition $[2ligand+2Zn+3OTf]^{1+}$.

The ions at m/z 1771, 1291, 1003, and 674, which contain (at least partly) hexazinc complexes carrying ligand **2** and 3+, 4+, 5+, or 7+ charges, respectively (cf., Table S2), were selected for IM separation. Five species are detected after dispersion of the

components of m/z 1771 by their ion mobilities (Figure 2a). Their isotope patterns (see insets in Figure 2a) reveal the presence of four different overlapping charge states, having isotope spacings (Δm) of 1.0, 0.50, 0.33, and 0.25 amu which diagnose ions with 1+, 2+, 3+, and 4+ charges, respectively. The signals at 13.81 (1+) and 8.59 (2+) ms must arise from ions with 2 and 4 bis(terpyridine)$-Zn^{II}$ units (cf., Table S2) and, thus, correspond to the linear fragments $L2^{1+}$ and $L4^{2+}$, respectively. On the other hand, the signals at 6.86 and 6.14 ms are due to hexameric complexes with 3+ charges (Table S2). It has been well documented that compact ions drift faster, while more extended structures drift more slowly in IM experiments.[38−47,50,55] This trend was confirmed in our study of hexameric <tpy−Cd^{II}−tpy> complexes, in which the macrocyclic (i.e., compact) isomer exhibited a consistently shorter drift time through the IM region than the linear (i.e., more extended) isomer.[47] Accordingly, the ions drifting at 6.86 and 6.14 ms, both of which have the same isotope spacing of Δm = 0.33 amu, were assigned to the linear ($L6^{3+}$) and cyclic ($C6^{3+}$) hexazinc complexes, respectively. The ions drifting at 5.14 ms show an isotope spacing of Δm = 0.25 amu and, hence, are either $L8^{4+}$, $C8^{4+}$, or an unresolved mixture of both these octameric architectures. Finally, the peak shoulder noticed at ∼7.7 ms gives rise to the same isotope pattern as $L6^{3+}$ and could originate from a small population of linear hexameric species (3+) with a conformation more extended than that of the major $L6^{3+}$ fraction.

The IM separation of m/z 1291 reveals the presence of three overlapping components in the 3−9 ms window (Figure 2b). On the basis of their isotope distributions and the corresponding drift times, the signal at 7.26 ms was assigned to $L3^{2+}$ and the signals at 5.20 and 4.56 ms (which show identical isotope spacings) to $L6^{4+}$ and $C6^{4+}$, respectively. The ions at m/z 1003 (Figure 2c) and 674 (Figure 2d) can only have one composition, viz., $M6^{5+}$ and $M6^{7+}$, respectively (cf., Table S2). Both these ions give two peaks after IM separation, which should arise from the corresponding linear and cyclic architectures; the hexameric isomers with 5+ charges (Figure 2c) are observed at 5.40 ($L6^{5+}$) and 4.37 ms ($C6^{5+}$), while those with 7+ charges (Figure 2d) are observed at 2.89 ($L6^{7+}$) and 2.18 ms ($C6^{7+}$). It is noteworthy that hexamers with the labile <tpy−Cd^{II}−tpy> connectivity could be adequately resolved by IM MS only in charge state 4+;[47] in contrast, the stronger <tpy−Zn^{II}−tpy> bonding permits satisfactory separation of linear and cyclic hexamers in charge states 3+, 4+, 5+, and 7+ (Figure 2). Interestingly, the separation between linear and cyclic isomers improves with the number of charges in the complex, presumably because increased charge repulsion enlarges more severely the collision cross-sections of linear than cyclic structures.

Identification of Penta-, Hexa-, and Heptameric Macrocycles. In order to obtain conclusive evidence that the pentamers, hexamers, and heptamers from library **2** contain macrocyclic architectures, the IM MS data of these n-mers were compared to those of analogous n-mers from library **3** (cf., Scheme 1). The bis(terpyridine) ligand **3** is a constitutional isomer of ligand **2**; it has a 180°-angle between the metal binding sites and, hence, forms purely linear complexes, which can serve, as standards, in establishing the structure(s) of the complexes in library **2**. A similar strategy was employed previously to differentiate linear and cyclic hexacadmium constructs.[47]

Two species with 4+ charges are detected at m/z 1051 for the pentamer from library **2** (Figure 3a, top). In contrast, only one 4+ ion is observed at m/z 1051 for the pentamer from library **3** (Figure 3a, bottom); the latter ion must be $L5^{4+}$, as ligand **3** forms exclusively linear architectures. Further, the drift time of $L5^{4+}$ from library **3** (2.35 ms) should be longer than the drift time of $L5^{4+}$ from library **2**, because ligand **3** (180°-angle geometry) is

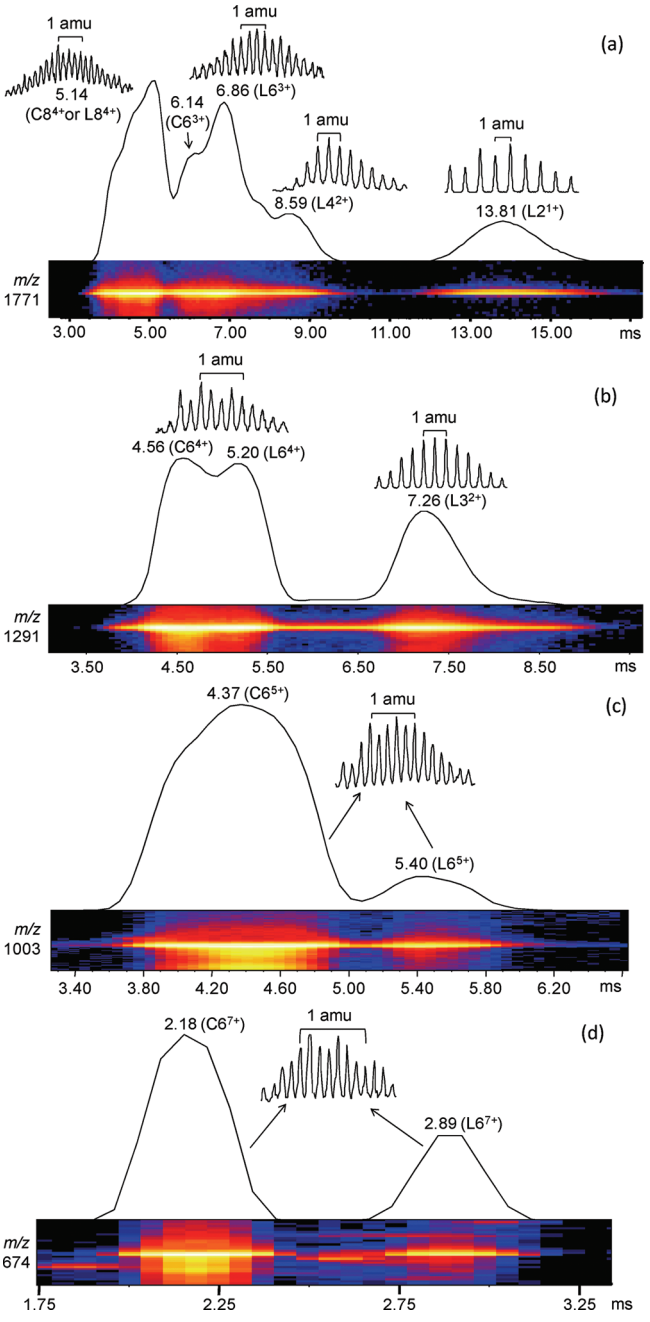

Figure 2. Two-dimensional IM MS plots (relative intensity vs drift time) of variously charged hexameric bis(terpyridine)$-Zn^{II}$ complexes from library **2**: (a) the ions appearing at m/z 1771 gave signals at 13.81, 8.59, 6.86, 6.14, and 5.14 ms, revealing the presence of superimposed $L2^{1+}$, $L4^{2+}$, $L6^{3+}$, $C6^{3+}$, and $L8^{4+}/C8^{4+}$ stoichiometries, respectively; (b) the ions at m/z 1291 gave signals at 7.26, 5.20, and 4.56 ms, corresponding to $L3^{2+}$, $L6^{4+}$, and $C6^{4+}$, respectively; (c) the ions at m/z 1003 gave signals at 5.40 and 4.37 ms, corresponding to $L6^{5+}$ and $C6^{5+}$, respectively; (d) the ions at m/z 674 gave signals at 2.89 and 2.18 ms, corresponding to $L6^{7+}$ and $C6^{7+}$, respectively. IM separation was performed using a traveling wave velocity of 350 m/s; the traveling wave height was 9.5 V for plots a and b and 8.5 V for plots c and d.

dx.doi.org/10.1021/ac201161u |*Anal. Chem.* 2011, 83, 6667–6674

Scheme 1. Synthetic Route to Libraries 1−3: (a) Reaction of 1−3 with $Zn(OTf)_2$ in $CHCl_3$/MeOH at 25 °C for 1 h

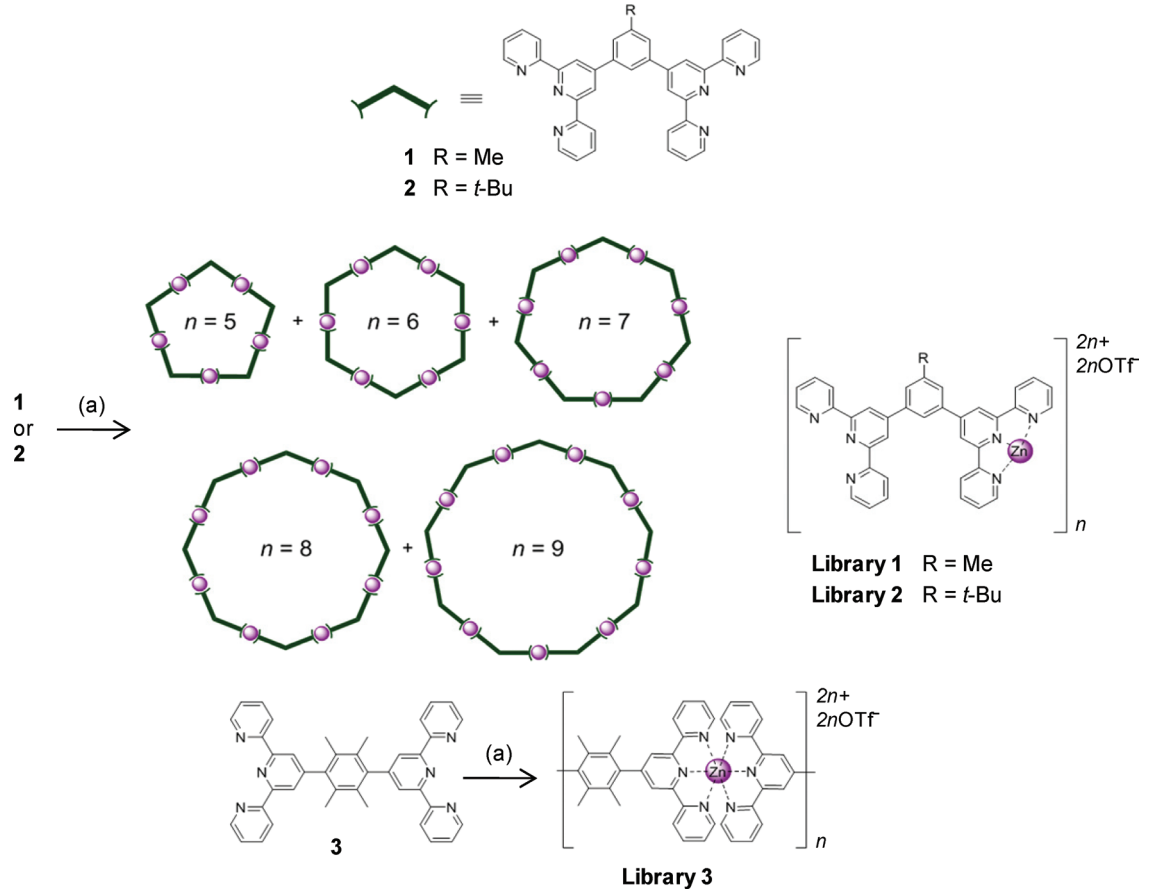

more extended in space than ligand **2** (120°-angle geometry). On the basis of these arguments, the fraction of m/z 1051 from library **2** drifting at 2.23 ms must be $L5^{4+}$, and the major fraction with the markedly shorter drift time of 1.78 ms must be $C5^{4+}$. Entirely analogous results were obtained for the hexamer (m/z 1291) and heptamer (m/z 1531) in charge state 4+. In either case, both linear and cyclic structures are present in the complexes of ligand **2** (Figures 3b and 3c, top), as confirmed by comparison with the corresponding products of ligand **3** (Figures 3b and 3c, bottom).

The drift times of the cyclic and linear isomers in library **2** increase from pentamer to heptamer, reflecting a concurrent increase of molecular size in this direction. A more quantitative description of the different complex sizes is provided by the corresponding collision cross-sections. The drift time scale of the traveling wave ion mobility device was calibrated using protein standards (see Figure S2 in Supporting Information), in order to convert the drift times of the cyclic and linear architectures of the library **2** complexes with five to seven repeat units and 4+ charges into experimental collision cross-sections; the results are listed in Table 1. Expectedly, the cross-sections of the more flexible and less compact linear isomers are larger. Since pentameric and heptameric Zn^{II} macrocycles with a 120°-angle ligand (**2**) had never been observed before, their structures and collision cross-sections were also examined computationally, together with those of the known hexamer. For each *n*-mer, 150 energy-minimized structures were generated by molecular mechanics/dynamics, and their collision cross-sections were calculated using the projection approximation method (cf., Figures S3−S5 in Supporting Information). The resulting average theoretical cross-sections are included in Table 1. No modeling was performed for the linear isomers, whose existence is not questioned. The experimental and theoretical collision cross-sections of C5, C6, and C7 agree well (all within ≤5%), substantiating the formation of such architectures upon self-assembly.

Identification of Octa- and Nonameric Macrocycles. The identification of macrocyclic pentamers, hexamers, and heptamers from library **2** was straightforward, as only two isomeric architectures were observed for each of these *n*-mers after ion mobility separation. The characterization of octameric and nonameric macrocycles (library **2**) becomes more complicated, because these oligomers show three or more isomeric/conformeric peaks in their IM MS plots (Figure 4). Here, spectral interpretation was aided by the IM MS data of the standards from library **3**, which are confined to extended linear structures due to the 180° angle in their Zn^{II} binding ligand, as well as by computational predictions about the order of collision cross-sections (and, hence, order of drift times) expected for the cyclic and linear isomers/conformers of the octamer (Figures S6 and S7 in Supporting Information) and nonamer (Figures S8 and S9 in Supporting Information). Previous studies showed that collision cross-sections are not affected significantly by the number of counterions (i.e., by charge state) in small *n*-mers[50] and very rigid assemblies[52] but may vary substantially with charge state in larger, more flexible complexes.[26,60] Furthermore, collision cross-sections calculated from energy-minimized structures by the most commonly

dx.doi.org/10.1021/ac201161u |*Anal. Chem.* 2011, 83, 6667–6674

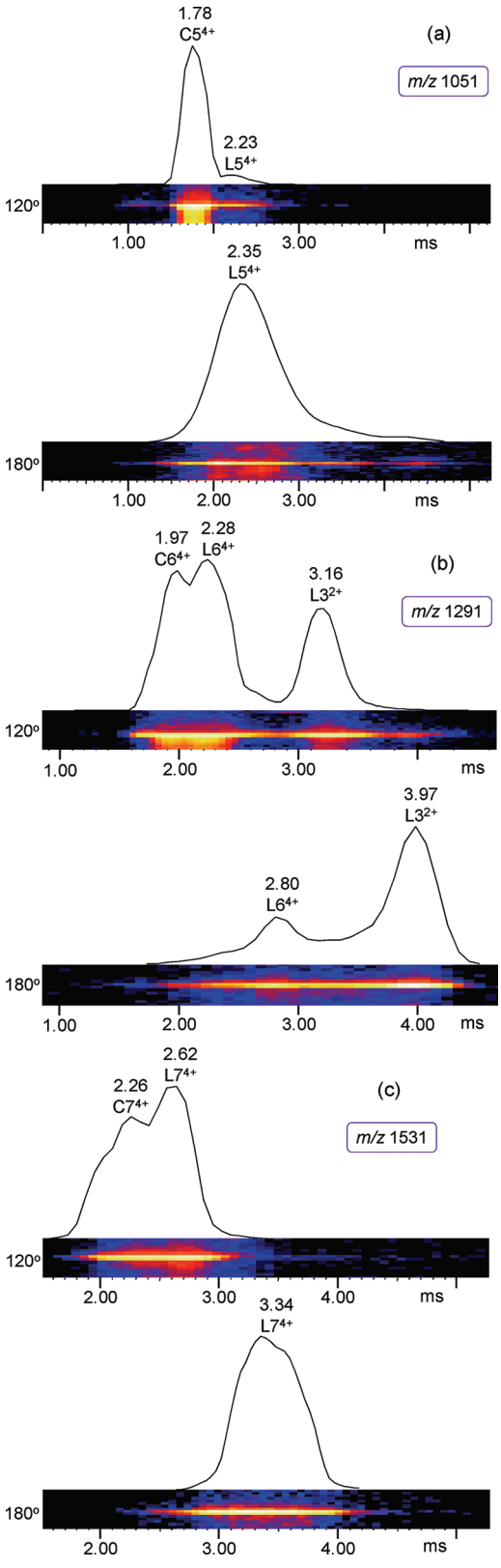

Figure 3. Two-dimensional IM MS plots of quadruply charged (a) pentameric, (b) hexameric, and (c) heptameric bis(terpyridine)−Zn^{II} complexes from library **2** (top traces) and library **3** (bottom traces); library **2** contains the 120°-angle ligand **2**, and library **3** the 180°-angle ligand **3**. IM separation was performed using a traveling wave velocity of 350 m/s and a traveling wave height of 12 V.

Table 1. Collision Cross-Sections (CCSs) of Pentameric, Hexameric, and Heptameric Bis(terpyridine)−Zn^{II} Complexes from Library 2

	CCS (Å^2)		
	experimental		theoretical
	macrocycle	linear isomer	macrocycle
pentamer	652 (C5)	693 (L5)	620 (C5)
hexamer	775 (C6)	832 (L6)	749 (C6)
heptamer	975 (C7)	1117 (L7)	938 (C7)

utilized projection approximation method may be underestimated for larger complexes; more accurate data are obtained by elaborate, less tractable trajectory calculations,[61,62] which were beyond the scope of the present investigation. Because of these reasons, the cross-sections obtained from modeling with the projection approximation approach (Figures S6−S9) were used only qualitatively, viz., to determine the order of drift times expected for the various octameric and nonameric architectures.

The ion at m/z 1386 from library **2** gave three resolved peaks after IM separation, centering at 1.53, 2.26, and 2.80 ms (cf., Figure 4a, top); the corresponding isotope distributions (not shown) indicate that all three peaks arise from octameric assemblies with 5+ charges ($M8^{5+}$). The standard from library **3** exhibited one isomer, $L8^{5+}$, drifting out at 2.98 ms (cf., Figure 4a, bottom); as mentioned above, this $L8^{5+}$ has an extended linear geometry. Therefore, the species from library **2** observed at the very similar drift time of 2.80 ms (1128 Å^2) should be the extended ring-opened octamer, $L8^{5+}$(extended). The other two signals at 1.53 and 2.26 ms could be cyclic or compact ring-opened octamers. Theory reveals the existence of macrocyclic (Figure S6) as well as linear isomers with folded, compact, and extended architectures (Figure S7). On the basis of the theoretically predicted cross-section order, the species drifting at 1.53 ms (802 Å^2) should be the folded ring-opened conformer, $L8^{5+}$(folded), while the species drifting at 2.26 (1035 Å^2) is a mixture of cyclic, $C8^{5+}$, and compact ring-opened, $L8^{5+}$(compact), isomers. Since the chain ends of $L8^{5+}$(compact) are very close to each other (cf., Figure S7), cyclization of this isomer to the thermodynamically most stable macrocyclic structure $C8^{5+}$, in which all Zn^{II} ions are optimally coordinated by two tpy ligands, should be facile.

Following the procedure used above for the octamer, the signal observed at 3.79 ms (1246 Å^2) for the nonamer from library **2** (Figure 4b, top) was assigned to the extended ring-opened conformer, $L9^{5+}$(extended), because its drift time is very similar with the 3.88-ms time observed for the linear $L9^{5+}$ complex from library **3** (Figure 4b, bottom). The modeling data for the nonamer isomers/conformers (Figures S8 and S9) predict that collision cross-sections increase in the order L9(folded) < L9(compact) < C9(cyclic) < L9(extended). Accordingly, the species drifting out at 2.08, 2.50, and 2.89 ms are attributed to $L9^{5+}$(folded), $L9^{5+}$(compact), and $C9^{5+}$, respectively.

Can Cyclic Architectures Be Formed in the Gas Phase? Although different macrocycles were detected and identified by IM MS, it is not a priori clear whether these macrocyclic architectures were already present in the solutions analyzed or whether they were created in the gas phase. This issue was probed by tandem mass spectrometry (MS^2) using members of

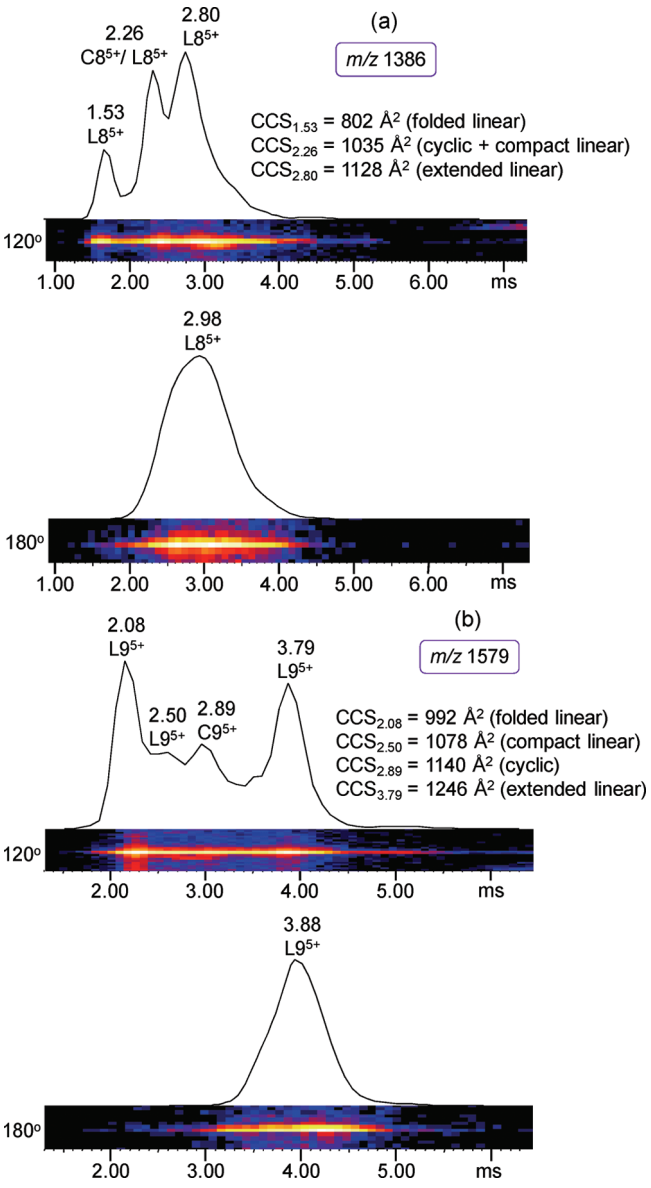

Figure 4. Two-dimensional IM MS plots of (a) octameric and (b) nonameric bis(terpyridine)−Zn^{II} complexes with 5+ charges from library **2** (top traces) and library **3** (bottom traces); library **2** contains the 120°-angle ligand **2**, and library **3** the 180°-angle ligand **3**. IM separation was performed using a traveling wave velocity of 350 m/s and a traveling wave height of 12 V. The collision cross-sections given for the architectures of library **2** (top traces) are experimental values deduced from the measured drift times.

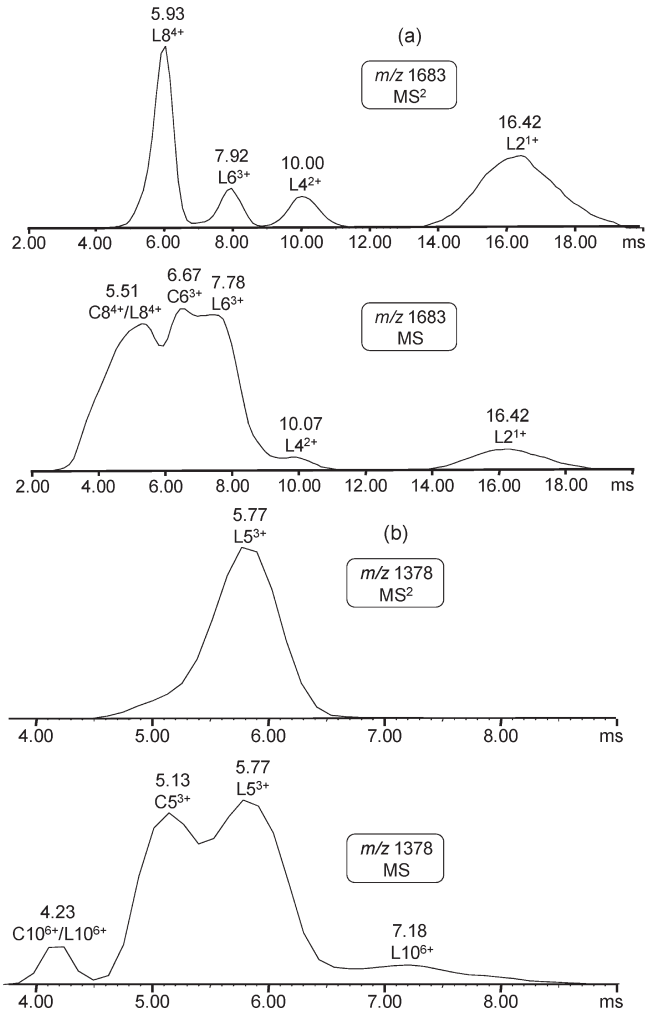

Figure 5. The top spectra in panels a and b show the IM-separated components of (a) m/z 1683 and (b) m/z 1378 formed by CAD of m/z 1454 ($C7^{4+}/L7^{4+}$) from library **1** (MS^2 mode). The bottom spectra in (a) and (b) show the IM-separated components of (a) m/z 1683 and (b) m/z 1378 formed in the ESI source (MS mode). In both cases, IM separation was performed at a traveling wave velocity of 350 m/s and a traveling wave height of 8.5 V.

library **1**. The ions at m/z 1378, 1683, and 1454 mainly contain cyclic and linear isomers of the pentameric ($C5^{3+}/L5^{3+}$), hexameric ($C6^{3+}/L6^{3+}$), and heptameric ($C7^{4+}/L7^{4+}$) complexes, respectively, as attested by the IM MS plots in Figure S10 in Supporting Information. The heptamer (m/z 1454), which is not contaminated by isobaric stoichiometries, was subjected to CAD. Dissociation of $C7^{4+}/L7^{4+}$ (m/z 1454) mainly yields fragments at m/z 1683 and 1378 (cf., Figure S11 in Supporting Information), whose components were separated by their ion mobilities and recorded in the IM MS^2 spectra depicted in the top traces shown in Figures 5a and 5b, respectively; note that all ions in these IM MS^2 spectra were generated in the gas phase. The bottom traces of Figures 5a and 5b show the IM MS plots of m/z 1683 and 1378, respectively, which include ions formed from the solutions fed to the ESI source. The hexameric $[6ligand+6Zn]^{3+}$ fragment generated by MS^2 (CAD) drifts out at 7.92 ms (cf., Figure 5a, top); this drift time agrees very well (within <2%) with the drift time of $L6^{3+}$ in the IM MS spectrum (7.78 ms; cf., Figure 5a, bottom) and is markedly different from the drift time of $C6^{3+}$ in the IM MS spectrum (6.67 ms). Also the drift time of the pentameric $[5ligand+5Zn]^{3+}$ fragment formed by MS^2 (CAD) drifts out at a time (5.77 ms; cf., Figure 5b, top) that matches the drift time of source-generated $L5^{3+}$ (5.77 ms; cf., Figure 5b, bottom) but differs substantially from the drift time of source-generated $C5^{3+}$ (5.13 ms). The shoulder on the left side of the $L5^{3+}$ signal (Figure 5b, top) could originate from a minor admixture of the corresponding compact linear pentamer and/or $C5^{3+}$. Overall, the proportion of cyclic fragments in the IM MS^2 spectra (Figures 5a and 5b, top) is negligible, providing strong evidence that the macrocyclic libraries observed in the IM mass spectra (Figures 5a and 5b, bottom) were already formed in the

solutions analyzed by ESI. The comparison of IM MS and IM MS^2 data also shows that CAD ("heating") disfavors the formation of cyclic fragments, probably due to entropy effects.

CONCLUSIONS

Oligomeric circular complexes with the stoichiometry <tpy−Zn−tpy>$_n$(OTf)$_{2n}$ ($n \geq 5$) are easily formed by Zn^{II}-mediated self-assembly of 120°-juxtaposed bis(terpyridine) ligands. The labile tpy−Zn^{II} bonds restrict, however, control over the product composition and generally lead to libraries of stoichiometries, which cannot generally be purified or separated by traditional chromatography methods for unequivocal spectroscopic characterization. Here, we showed how the penta- to nonameric macrocycle constituents of these libraries can be isolated and conclusively identified using IM MS and IM MS^2. These methods blend gas-phase chromatographic dispersion with composition and structure determination by MS and MS^2, allowing one to probe individual mixture constituents selected from the raw product by their size, charge, and shape. Differentiation of the architectures formed during self-assembly was facilitated by using reference standards formed from isomeric 180°-angle building blocks which, unlike the 120°-angle ligands, can only render linear structures. Additional help was provided by modeling of the shapes (collision cross-sections) of isomeric architectures to predict the order of their drift times ("elution times") through the ion mobility region for comparison with the experimentally observed drift time orders. Finally, tandem mass spectrometry was interfaced with ion mobility separation to ascertain that cyclic structures are not formed during collision-activated fragmentation in the gas phase and that all macrocycles observed in the IM MS experiments were already formed in solution. The approach described in this work should be of value in the characterization of supramolecular combinatorial libraries yielding mixtures of *n*-mers, isomers, and conformers that are not amenable to regular LC-MS (MS^2) studies or to NMR and X-ray spectroscopic analyses (which presuppose pure, single compounds).

ASSOCIATED CONTENT

Supporting Information. Additional information as noted in the text. This material is available free of charge via the Internet at http://pubs.acs.org.

AUTHOR INFORMATION

Corresponding Author

*Fax: (330) 972-6085. E-mail: wesdemiotis@uakron.edu; newkome@uakron.edu.

ACKNOWLEDGMENT

The authors gratefully acknowledge support from the National Science Foundation (DMR-0705015 and 0812337 to G.R. N.; DMR-0821313 and CHE-1012636 to C.W.).

REFERENCES

(1) Lehn, J.-M. *Supramolecular Chemistry: Concepts and Perspectives*; VCH: Weinheim, 1995.
(2) Lehn, J.-M. *Chem.—Eur. J.* **1999**, *5*, 2455–2463.
(3) Fujita, M.; Yazaki, J.; Ogura, K. *J. Am. Chem. Soc.* **1990**, *112*, 5645–5647.
(4) Fujita, M.; Sasaki, O.; Mitsuhashi, T.; Fujita, T.; Yazaki, J.; Yamaguchi, K.; Ogura, K. *Chem. Commun.* **1996**, 1535–1536.
(5) Romero, F. M.; Ziessel, R.; Dupont-Gervais, A.; Van Dorsselaer, A. *Chem. Commun.* **1996**, 551–553.
(6) Hasenknopf, B.; Lehn, J.-M.; Kneisel, B. O.; Baum, G.; Fenske, D. *Angew. Chem., Int. Ed. Engl.* **1996**, *35*, 1838–1840.
(7) Baxter, N. W.; Lehn, J.-M.; Rissanen, K. *Chem. Commun.* **1997**, 1323–1324.
(8) Hasenknopf, B.; Lehn, J.-M.; Boumediene, N.; Dupont-Gervais, A.; Van Dorsselaer, A.; Kneisel, B.; Fenske, D. *J. Am. Chem. Soc.* **1997**, *119*, 10956–10962.
(9) Lee, S. B.; Hwang, S.; Chung, D. S.; Yun, H.; Hong, J. I. *Tetrahedron Lett.* **1998**, *39*, 873–876.
(10) Ma, G.; Jung, Y. S.; Chung, D. S.; Hong, J. I. *Tetrahedron Lett.* **1999**, *40*, 531–534.
(11) Hiraoka, S.; Fujita, M. *J. Am. Chem. Soc.* **1999**, *121*, 10239–10240.
(12) Mamula, O.; Monlien, F. J.; Porquet, A.; Hopfgartner, G.; Merbach, A.; von Zelewsky, A. *Chem.—Eur. J.* **2001**, *7*, 533–539.
(13) Kraus, T.; Budesinsky, M.; Cvacka, J.; Sauvage, J.-P. *Angew. Chem., Int. Ed.* **2006**, *45*, 258–261.
(14) Suzuki, K.; Kawano, M.; Fujita, M. *Angew. Chem., Int. Ed.* **2007**, *46*, 2819–2822.
(15) Schubert, U. S.; Winter, A.; Newkome, G. R. *Terpyridine-based Materials - For Catalytic, Optoelectronic and Life Science Applications*; Wiley-VCH: Weinheim, 2011.
(16) Hasenknopf, B.; Lehn, J. M.; Baum, G.; Fenske, D. *Proc. Natl. Acad. Sci. U.S.A.* **1996**, *93*, 1397–1400.
(17) Huc, I.; Lehn, J.-M. *Proc. Natl. Acad. Sci. U.S.A.* **1997**, *94*, 2106–2110.
(18) Goral, V.; Nelen, M. I.; Eliseev, A. V.; Lehn, J.-M. *Proc. Natl. Acad. Sci. U.S.A.* **2001**, *98*, 1347–1352.
(19) Provent, C.; Rivara-Minten, E.; Hewage, S.; Brunner, G.; Williams, A. F. *Chem.—Eur. J.* **1999**, *5*, 3487–3494.
(20) Senegas, J. M.; Koeller, S.; Bernardinelli, G. R.; Piguet, C. *Chem. Commun.* **2005**, 2235–2237.
(21) Newkome, G. R.; Cho, T. J.; Moorefield, C. N.; Baker, G. R.; Saunders, M. J.; Cush, R.; Russo, P. S. *Angew. Chem., Int. Ed.* **1999**, *38*, 3717–3721.
(22) Newkome, G. R.; Cho, T. J.; Moorefield, C. N.; Cush, R.; Russo, P. S.; Godinez, L. A.; Saunders, M. J.; Mohapatra, P. *Chem.—Eur. J.* **2002**, *8*, 2946–2954.
(23) Newkome, G. R.; Cho, T. J.; Moorefield, C. N.; Mohapatra, P. P.; Godinez, L. A. *Chem.—Eur. J.* **2004**, *10*, 1493–1500.
(24) Hwang, S.-H.; Moorefield, C. N.; Wang, P.; Kim, J.-Y.; Lee, S.-W.; Newkome, G. R. *Inorg. Chim. Acta* **2007**, *360*, 1780–1784.
(25) Chan, Y.-T.; Moorefield, C. N.; Soler, M.; Newkome, G. R. *Chem.—Eur. J.* **2010**, *16*, 1768–1771.
(26) Chan, Y.-T.; Li, X.; Moorefield, C. N.; Wesdemiotis, C.; Newkome, G. R. *Chem.—Eur. J.* **2011**, *17*, 7750–7754.
(27) Chan, Y.-T.; Li, X.; Yu, J.; Carri, G. A.; Moorefield, C. N.; Newkome, G. R.; Wesdemiotis, C. *J. Am. Chem. Soc.* **2011**, *133*, 11967–11976.
(28) Ghosh, K.; Hu, J.; White, H. S.; Stang, P. J. *J. Am. Chem. Soc.* **2009**, *131*, 6695–6697.
(29) Lee, J.; Ghosh, K.; Stang, P. J. *J. Am. Chem. Soc.* **2009**, *131*, 12028–12029.
(30) Lusby, P. J.; Müller, P.; Pike, S. J.; Slawin, A. M. Z. *J. Am. Chem. Soc.* **2009**, *131*, 16398–16400.
(31) Mahata, K.; Schmittel, M. *J. Am. Chem. Soc.* **2009**, *131*, 16544–16554.
(32) Sato, S.; Ishido, Y.; Fujita, M. *J. Am. Chem. Soc.* **2009**, *131*, 6064–6065.
(33) Suzuki, K.; Kawano, M.; Fujita, M. *Chem. Commun.* **2009**, 1638–1640.
(34) Zheng, Y. R.; Stang, P. J. *J. Am. Chem. Soc.* **2009**, *131*, 3487–3489.
(35) Jiang, W.; Schafer, A.; Mohr, P. C.; Schalley, C. A. *J. Am. Chem. Soc.* **2010**, *132*, 2309–2320.
(36) Sun, Q. F.; Iwasa, J.; Ogawa, D.; Ishido, Y.; Sato, S.; Ozeki, T.; Sei, Y.; Yamaguchi, K.; Fujita, M. *Science* **2010**, *328*, 1144–1147.

(37) Wang, M.; Zheng, Y. R.; Ghosh, K.; Stang, P. J. *J. Am. Chem. Soc.* **2010**, *132*, 6282–6283.
(38) Bowers, M. T.; Kemper, P. R.; von Helden, G.; van Koppen, P. A. M. *Science* **1993**, *260*, 1446–1451.
(39) Clemmer, D. E.; Jarrold, M. F. *J. Mass Spectrom.* **1997**, *32*, 577–592.
(40) Hoaglund-Hyzer, C. S.; Counterman, A. E.; Clemmer, D. E. *Chem. Rev.* **1999**, *99*, 3037–3079.
(41) Verbeck, G. F.; Ruotolo, B. T.; Sawyer, H. A.; Gillig, K. J.; Russel, D. H. *J. Biomol. Tech.* **2002**, *13*, 56–61.
(42) Trimpin, S.; Plasencia, M.; Isailovic, D.; Clemmer, D. E. *Anal. Chem.* **2007**, *79*, 7965–7974.
(43) Fenn, L. S.; McLean, J. A. *Anal. Bioanal. Chem.* **2008**, *391*, 905–909.
(44) Kanu, A. B.; Dwivedi, P.; Tam, M.; Matz, L.; Hill, H. H. *J. Mass Spectrom.* **2008**, *43*, 1–22.
(45) Ruotolo, B. T.; Benesch, J. L. P.; Sandercock, A. M.; Hyung, S. J.; Robinson, C. V. *Nat. Protocols* **2008**, *3*, 1139–1152.
(46) Trimpin, S.; Clemmer, D. E. *Anal. Chem.* **2008**, *80*, 9073–9083.
(47) Chan, Y.-T.; Li, X.; Soler, M.; Wang, J.-L.; Wesdemiotis, C.; Newkome, G. R. *J. Am. Chem. Soc.* **2009**, *131*, 16395–16397.
(48) Perera, S.; Li, X.; Soler, M.; Schultz, A.; Wesdemiotis, C.; Moorefield, C. N.; Newkome, G. R. *Angew. Chem., Int. Ed.* **2010**, *49*, 6539–6544.
(49) Ren, X.; Sun, B.; Tsai, C. C.; Tu, Y.; Leng, S.; Li, K.; Kang, Z.; Horn, R. M. V.; Li, X.; Zhu, M.; Wesdemiotis, C.; Zhang, W. B.; Cheng, S. Z. D. *J. Phys. Chem. B* **2010**, *114*, 4802–4810.
(50) Brocker, E. R.; Anderson, S. E.; Northrop, B. H.; Stang, P. J.; Bowers, M. T. *J. Am. Chem. Soc.* **2010**, *132*, 13486–13494.
(51) Perera, S.; Li, X.; Guo, M.; Wesdemiotis, C.; Moorefield, C. N.; Newkome, G. R. *Chem. Commun.* **2011**, *47*, 4658–4660.
(52) Wang, J.-L.; Li, X.; Lu, X.; Hsieh, I.-F.; Cao, Y.; Moorefield, C. N.; Wesdemiotis, C.; Chang, S. Z. D.; Newkome, G. R. *J. Am. Chem. Soc.* **2011**, *133*, 11450–11453.
(53) Pringle, S. D.; Giles, K.; Wildgoose, J. L.; Williams, J. P.; Slade, S. E.; Thalassinos, K.; Bateman, R. H.; Bowers, M. T.; Scrivens, J. H. *Int. J. Mass Spectrom.* **2007**, *261*, 1–12.
(54) Thalassinos, K.; Grabenauer, M.; Slade, S. E.; Hilton, G. R.; Bowers, M. T.; Scrivens, J. H. *Anal. Chem.* **2009**, *81*, 248–254.
(55) Li, X.; Chan, Y.-T.; Newkome, G. R.; Wesdemiotis, C. *Anal. Chem.* **2011**, *83*, 1284–1290.
(56) Smiljanic, D.; Wesdemiotis, C. *Int. J. Mass Spectrom.* **2011**, *204*, 148–153.
(57) Angel, L. A.; Majors, L. T.; Dharmaratne, A. C.; Dass, A. *ACS Nano* **2010**, *4*, 4691–4700.
(58) Li, X.; Guo, L.; Casiano-Maldonado, M.; Zhang, D.; Wesdemiotis, C. *Macromolecules* **2011**, *44*, 4555–4564.
(59) Hamilton, J. M.; Anhorn, M. J.; Oscarson, K. A.; Reibenspies, J. H. *Inorg. Chem.* **2011**, *50*, 2764–2770.
(60) Wang, J.-L.; Li, X.; Lu, X.; Chan, Y.-T.; Moorefield, C. N.; Wesdemiotis, C.; Newkome, G. R. *Chem.—Eur. J.* **2011**, *17*, 4830–4838.
(61) Mesleh, M. F.; Hunter, J. M.; Shvartsburg, A. A.; Schatz, G. C.; Jarrold, M. F. *J. Phys. Chem.* **1996**, *100*, 16082–16086.
(62) Shvartsburg, A. A.; Jarrold, M. F. *Chem. Phys. Lett.* **1996**, *261*, 86–91.